RESEARCH ARTICLE

Characterisation of copal resin and amber by negative-ion electrospray ionisation Fourier transform ion cyclotron resonance mass spectrometry

Yankuan Tian[1] | Jia-Nan Sun[1,2] | Bin Jiang[1] | Zhao-Wen Zhan[1]

[1]State Key Laboratory of Organic Geochemistry, Guangzhou Institute of Geochemistry, Chinese Academy of Sciences, Guangzhou, China

[2]University of Chinese Academy of Sciences, College of Earth and Planetary Sciences, Beijing, China

Correspondence
Zhao-Wen Zhan, State Key Laboratory of Organic Geochemistry, Guangzhou Institute of Geochemistry, Chinese Academy of Sciences, Guangzhou 510640, China.
Email: zhanzw@gig.ac.cn

Abstract

Copal resin and amber from Columbia were analysed by negative-ion electrospray ionisation (ESI) Fourier transform ion cyclotron resonance mass spectrometry (FT-ICR MS), with particular focus on polar compounds with relatively high molecular weights. A total of 4038 and 2755 compounds were identified between m/z 150 and 1,000 in the spectra of the copal resin and amber DCM extracts, respectively. The CHO classes were the most abundant species in the detected polar compounds. The petrochemical process of converting copal resin to amber is accompanied by evaporation and dispersion of volatile molecules and polymerisation of relatively smaller molecules. Thus, the most abundant compounds in copal resin comprised more than one C_5 basic unit compared to amber, and the relative abundances of compounds with a high number of carbon and oxygen atoms in amber were higher than those in copal resin. There were strong positive correlations between the double-bond equivalence (DBE_{av}) values and the number of oxygen atoms in both samples. The slopes and y-intercepts of the linear relationship indicated that the C_5 pentadienoic acid is the basic structure of heteroatom compound molecules in copal resin and amber. FT-ICR MS analysis focuses on the characterisation of heteroatom compounds with relatively high molecular weight and is helpful to provide supplementary information on the origin and evolution of complex organic mixtures such as copal resin and amber at the molecular level in a fast and convenient way.

KEYWORDS
amber, copal resin, DBE, FT-ICR MS, oxygenated compounds

1 | INTRODUCTION

Copal resin is an extremely complex and diverse mixture that was secreted by certain kinds of plants, primarily the genus *pinus*, from the Cretaceous period to the Cenozoic Tertiary. Amber is the polymerised and fossilised remains of plant resins. Both are composed of C, H, O, N, etc., and trace metal elements. They mainly contain volatile or nonvolatile terpenoid compounds and secondary compounds of phenol. They have some similarities in terms of their physical and chemical properties, whereas different maturities led to some differences.

Beyond their ornamental value, amber is a marker of the origin and evolution of terrestrial plants, and inclusions entrapped in resin and amber often preserve some animal or vegetal species that are frequently extinct. Analysis of the chemical composition of plant resins and amber provides information about their botanical origin and place of production, information that is helpful in studying the evolutionary history of life on earth and climatic/geological changes.

Several analytical techniques have been applied to characterise the chemical composition of amber and plant resin. Solid-state spectroscopic techniques such as infrared spectroscopy, Raman

spectroscopy, and ^{13}C nuclear magnetic resonance (^{13}C NMR) have been applied to analyse the structural characteristics of amber and resins.[1-5] Fourier transform infrared spectroscopy has been widely used to study their chemical functional groups;[6] the detection of C=O and O–C=O groups helps determine the types of compounds. Worldwide, amber is classified into four groups according to its ^{13}C NMR spectra.[7-9] Gas chromatography–mass spectrometry (GC–MS) analysis of the extract fraction or the volatile components provides the distribution of individual compounds and their structural information.[10-13] Furthermore, the biomarker distribution contained in plant resin and amber can be obtained from the GC–MS analysis, providing valuable information on the specific plant source and related climate and origin information.[14] However, chemical derivatisation is often required for GC–MS analysis of the polar extracts of amber or resins.[15] GC–MS gives only the low-molecular-weight fraction, such as di- and tri-terpenoid compounds, and the polar non-volatile heteroatomic compounds, that is, nitrogen-, sulphur-, and oxygen-containing (NSO) compounds; polymers are usually ignored. Pyrolysis-GC–MS (Py-GC–MS) is a unique technique that yields more detailed and specific information on the polymeric structure of the insoluble part of amber and copal resin.[16] Bray et al.[17] used Py-GC–MS to analyse the terpene distribution in Early Cretaceous (Barremian) amber (fossil resin) and obtain useful chemotaxonomic data.

The ultrahigh resolution and accuracy of Fourier transform ion cyclotron resonance mass spectrometry (FT-ICR MS) provide a novel and effective method to analyse complex mixtures and identify the chemical formulae of the detected masses.[18] The combination of electrospray ionisation (ESI) allows soft ionisation for analysing polar components in complex mixtures. In addition, negative-ion ESI FT-ICR MS can detect compounds with higher molecular weights (500–1200 Da) in natural organic matter compared to traditional GC–MS, by which usually only compounds with molecular weights less than m/z 300 were detected a mass range of 50–500 Da. It allows direct FT-ICR MS analysis without chemical derivatisation. Oxygen-containing compounds such as acids and phenols in copal resin and amber are easily ionised and analysed by negative-ion ESI FT-ICR MS.

Here, the dissolved organic matter of a copal resin and amber were analysed by ESI FT-ICR MS, with particular focus on the main polar compounds, that is, oxygen-containing compounds. The chemical compositions of the copal resin and amber were characterised and compared to explain the molecular composition changes that occurred during the transformation of copal resin to amber. This will help researchers understand their chemotaxonomic data and classification.

2 | SAMPLES AND EXPERIMENT

2.1 | Samples and FT-ICR MS analysis

Copal resin and amber from Columbia were chosen as typical samples. Both were taken from local mining sites. In the laboratory, clean samples were selected and ground to 200 mesh by hand. The powdered samples were extracted using ultrasound with dichloromethane (DCM). The procedures were repeated 2–3 times until the extracts were colourless. The extracts were then collected and prepared to the FT-ICR MS analysis.

Mass analyses of the above two extracts were performed in negative-ion ESI mode using a SolariX XR FT-ICR MS (Bruker Daltonik GmbH, Bremen, Germany) equipped with a 9.4 T refrigerated actively shielded superconducting magnet (Bruker Biospin, Wissembourg, France) and a Paracell analyser cell. ESI voltages were optimised at 3500 kV to maintain consistent and stable ion currents. The ions were accumulated for 0.008 s in an argon-filled collision cell before transferring to the ICR cell. A total of 128 continuous 4 M data FT-ICR transients were added to enhance the signal-to-noise ratio and the dynamic range. The mass range was 150–1200 Da.

The DCM extracts of the copal resin and amber were diluted to 0.001, 0.01, 0.10, 0.20 mg/mL with a DCM/methanol solution (1:3, v/v). Then, the diluted solutions were injected into the ESI ion source by a syringe pump operating at 180 μL/hr. The solutions with the concentration of 0.1 mg/mL were repeated three times at the same conditions. Methanol blank scanning was performed before each injection to reduce contamination and ensure the cleanliness of the system.

2.2 | Mass calibration and data quality control

The mass spectra were calibrated with a known series of alkyl O2 compounds that are abundant in petroleum samples in negative-ion ESI mode using a linear calibration. The final spectrum was internally recalibrated with typical O2-class species peaks in the samples using quadratic calibration in DataAnalysis 5.0 (Bruker Daltonics). A mass-resolving power ($m/\Delta m50\%$, where $\Delta m50\%$ is the magnitude of the mass spectral peak full-width at half-maximum peak height) > 450,000 at m/z 319 with <0.2 ppm absolute mass error was achieved. Data analysis was performed by custom software.[19] Only peaks with signal to noise ratio (S/N) greater than 4 were exported and are discussed in this text. Elemental formulae were calculated and assigned using a molecular formula calculator based on the m/z values within a 1-ppm error range.

The formula $C_cH_hO_oN_nS_s$ was used to indicate the assigned compounds, in which C, H, O, N, S indicate carbon, hydrogen, oxygen, nitrogen, and sulphur, respectively, and c, h, o, n, s represent the number of atoms of the respective elements. The maximum numbers of atoms for the formula calculator were set as follows: 50 ^{12}C, 20 ^{16}O, 1 ^{14}N, 1 ^{32}S, 1 ^{13}C, 1 ^{18}O and 1 ^{34}S. There is no limit to the number of hydrogen atoms, but the rules must be obeyed: $1/3^*c \leq h \leq (2c + n + 2)$ and $(h + n)$ must be even (the nitrogen rule).[20] The modified aromaticity index (AI_{mod}) and double-bond equivalence (DBE) based on calculation of the elemental composition were calculated to further characterise the assigned compounds. The intensity-weighted average molecular parameters were also calculated for each sample (Table 1). The identified formulae containing isotopomers are not discussed.

A series of concentrations of DCM extracts ranging from 0.001 to 0.2 mg/mL were analysed to evaluate the effect of concentration on the ionization efficiency. Generally, the injection concentration of 0.2 mg/mL is the most widely selected, especially for crude oil and

TABLE 1 Intensity-weighted average (wa) molecular parameters in the copal resin and amber

Sample	Copal resin	Amber	Formulas
No.	4038	2755	$C_cH_hO_oN_nS_s$
m/z_{wa}, Da	500.05	528.49	$\sum(m/z) \times I / \sum I$
C_{wa}	27.91	28.78	$\sum(\text{number of C}) \times I / \sum I$
H_{wa}	41.45	42.18	$\sum(\text{number of H}) \times I / \sum I$
O_{wa}	7.68	8.76	$\sum(\text{number of O}) \times I / \sum I$
N_{wa}	0.04	0.03	$\sum(\text{number of N}) \times I / \sum I$
H/C_{wa}	1.49	1.47	H_{wa}/C_{wa}
O/C_{wa}	0.27	0.30	O_{wa}/C_{wa}
DBE_{wa}	7.71	8.21	$\sum DBE \times I / \sum I$
$Almod_{wa}$	0.19	0.20	$\sum Almod \times I / \sum I$

Note: The C, H, O, N, S indicate carbon, hydrogen, oxygen, nitrogen and sulphur, respectively, and c, h, o, n, s represent the number of atoms of the respective elements. $\sum$ = sum; I = intensity; DBE = double-bond equivalence; Almod = modified aromaticity index = $(1 + c - 0.5o - s - 0.5 h)/(c - 0.5o - s - n)$.[26,27]

source rock extracts.[21–23] The results showed the characteristics of two peak groups on the broadband spectra over the concentration range, but low concentration injections (0.001 and 0.01 mg/mL) reduced detected compounds and the relative intensity (Figures S1 and S2). Considering high concentration may lead to the aggregation of low molecular weight compounds, the concentration of 0.1 mg/mL was finally adopted and repeatedly injected and analysed three times to investigate the stability of the system and the repeatability of data. Data qualities were characterised by the similar broadband spectrums of repeated injections (Figures S3 and S4) and good repeatability of relative peak intensity at m/z 305 and 617 and overall mass peaks of the copal resin and amber samples (Tables S1 and S2). Therefore, the mass spectrum data with 0.1-mg/mL injection concentration were used and discussed in this text.

3 | RESULTS AND DISCUSSIONS

3.1 | General characteristics

The negative-ion ESI FT-ICR MS broadband spectra of the DCM extracts of the copal resin and amber from Columbia are shown in Figure 1. Both spectra show that the molecular weight distributions of the DCM extracts of the copal resin and amber are mainly distributed
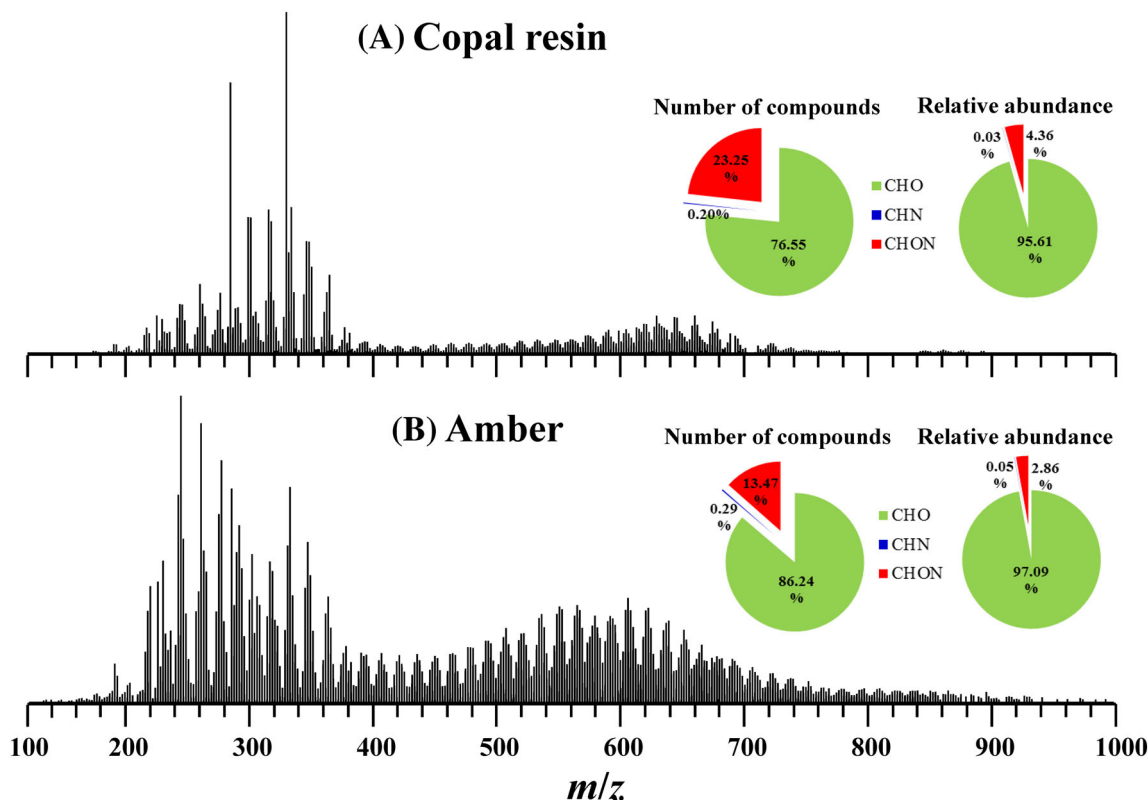

FIGURE 1 Negative-ion electrospray ionisation (ESI) Fourier transform ion cyclotron resonance mass spectrometry (FT-ICR MS) broadband spectra of the DCM extracts of the copal resin and amber from Columbia. The pie charts show the percentages (by number of compounds and by intensity) of the identified different classes of heteroatom compounds in each sample

between 150 and 800 Da, with two peak groups. The front is the main peak group, with an *m/z* range from 200 to 450 Da; the back is the secondary peak group, with an *m/z* range from 450 to 800 Da (Figure 1). The overall distribution pattern of the spectra and the approximate multiple relationships of molecular weight between the front and back peak groups indicate the presence of polymers in the two extracts. The main molecular weight distribution and relative abundance of the front and back peak groups were different in the two samples. The most abundant compound in the copal resin was $C_{20}H_{30}O_5$ (*m/z* = 349.20), and the second most abundant compound was $C_{20}H_{34}O_2$ (*m/z* = 305.24). The most abundant compounds in the amber were C_{15} series, with empirical formulae of $C_{15}H_{22}O_4$, $C_{15}H_{22}O_5$ and $C_{15}H_{22}O_6$. This abundance can be explained by the aromatisation and polymerisation reaction of terpane components during the transformation of copal resin to amber.[24] The relative abundance of the front peak group (*m/z* < 450 Da) in the copal resin was 46.17% (1303 compounds, 32.27%), whereas that of the back peak group (*m/z* = 450–800 Da) was 49.39% (2209 compounds, 54.71%). However, the relative abundance of the front peak group in the amber was 34.13% (813 compounds, 29.51%), whereas that of the back peaks group was 59.86% (1481 compounds, 53.76%). Compared with the copal resin, the molecular weight of the main compounds in the two peak groups decreased and the relative abundance of high-molecular-weight compounds increased in the amber. This may be due to the degradation and oxidisation of high-molecular-weight compounds, as they were exposed to air for longer periods of time during the conversion of copal resin to amber; the polymerisation of low-molecular-weight compounds may also have been a factor in the conversion process.

Some empirical parameters are helpful to further understand the molecular-level characteristics of the copal resin and amber. Table 1 shows the intensity-weighted average (wa) molecular parameters of the two samples. The average molecular weight (m/z_{wa}) of the amber was 528 Da, which is higher than that of the copal resin. The aromaticity index (AI), a conservative calculation method, is used to classify organic compounds with respect to their possible functional groups.[25] The modified AI (AI_{mod}), which assumes that half of the oxygen atoms in the molecule form a double bond, was used to identify the aromatic formulae.[26] Formulae with AI_{mod} < 0.5 were classified as mainly olefinic and aliphatic compounds. The AI_{mod} values of most compounds in the copal resin and amber were less than 0.5, and the $AI_{mod\ wa}$ values were 0.19 and 0.20, respectively, suggesting that the oxygen-containing compounds may be mainly composed of acids, alcohols, and aldehydes.[27] The close parameter values of the H/C_{wa} and O/C_{wa} ratios and $AI_{mod\ wa}$ in the two samples indicated that they had similar chemical compositions and origins (Table 1).

A total of 4038 and 2755 compounds were identified between *m/z* 150 and 1000 in the spectra from the copal resin and amber DCM extracts, respectively, excluding isotope peaks, suggesting that the copal resin had more soluble organic matter containing heteroatoms than the amber. Based on the accurate molecular weight of the mass spectrum peak, the identified compounds were classified according to the heteroatoms. S-containing compounds were not detected in either sample. In the copal resin, compounds with molecular formulae of CHO, CHN, and CHON were detected at 3091 (76.55%), 8 (0.20%) and 939 (23.25%), respectively, and their relative abundances were 95.61%, 0.03% and 4.36%, respectively. In the amber, the number of these compounds were 2376 (86.24%), 8 (0.29%) and 371(13.47%), respectively, with relative abundances of 97.07%, 0.05% and 2.86%, respectively (Figure 1). The CHO class was the most abundant species both in the copal resin and amber, which will be discussed in detail in the following sections.

3.2 | Van Krevelen analysis

Van Krevelen diagrams have been used to extract structural information and classify organic matter molecules into different biochemical class species based on the combination of their H/C, O/C and N/C atomic ratios and aromaticity indices. This is mainly because specific compound species have characteristic atomic ratios. According to the classification and evaluation criteria described and applied by previous studies,[27–29] van Krevelen diagram can be classified into seven regions: (1) lipid-like region (O/C = 0–0.2, H/C = 1.7–2.2); (2) protein/amino sugar-like region (O/C = 0.2–0.6, H/C = 1.5–2.2, N/C ≥ 0.05); (3) carbohydrate-like region (O/C = 0.6–1.2, H/C = 1.5–2.2); (4) unsaturated hydrocarbon-like region (O/C = 0–0.1, H/C = 0.7–1.5); (5) lignin-like region (O/C = 0.1–0.6, H/C = 0.6–1.7, AI_{mod} < 0.67); (6) tannin-like region (O/C = 0.6–1.2, H/C = 0.5–1.5, AI_{mod} < 0.67); and (7) condensed aromatic ring structure region (O/C = 0–1, H/C = 0.3–0.7, AI_{mod} ≥ 0.67).

Van Krevelen diagrams were plotted to better visualise the chemical compositions of the DCM extracts of the copal resin and amber (Figure 2). The H/C and O/C atomic ratios in the two samples were mainly distributed as 0.7–2.0 and 0–0.8, respectively. Although most regions in the plots were dotted with the formulae from the two samples, the van Krevelen analysis classified the copal resin and amber extracts mainly into two different biochemical classes (Figure 2). The lignin-like components were the most abundant, contributing 3250 peaks in the copal resin and 2260 peaks in the amber, accounting for 80.49% and 82.03%, respectively, of the total number of peaks. The second major class was the protein/amino sugar-like components, which included 349 (8.64%) and 282 (10.24%) peaks in the copal resin and amber, respectively. The tannin-like and lipid-like components were the lower-level ingredients, accounting for 3.12% and 3.02% of the amber peaks, respectively, and 2.40% and 2.14% of the copal peaks, respectively. These compound species are the main chemical components of higher plants, and they correlated well with previous work identifying these compounds in natural resins.[30,31] Although the amount of the heteroatom compounds detected in the DCM extracts of the copal resin and amber is quite different, the relative proportions of all kinds of compounds are very close, which also indicates that they have similar chemical compositions and origins. The difference between the two samples was the relative proportion of compounds with *m/z* > 700, especially in the protein/amino sugar-like components, indicating that different fossil inclusions may be entrapped and
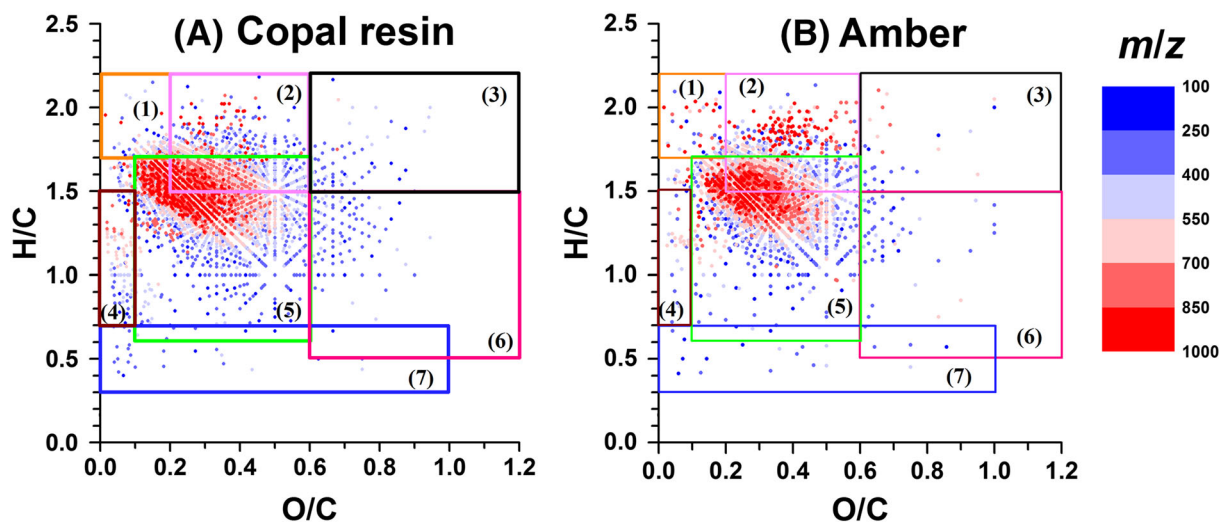
FIGURE 2 Van Krevelen diagrams for molecular formulas of the (a) copal resin and (b) amber assigned to the negative ion mode Fourier transform ion cyclotron resonance mass spectrometry (FT-ICR MS) spectral peaks. Boxes overlain on the diagrams indicate biomolecular compound classes based on the classification described by Lu et al.[27] and He et al.[29] the shared regions (overlapping boxes) are distinguished by N/C atomic ratio or modified aromaticity index[28]

that polymerisation may have occurred during the transformation from copal resin to amber.[32]

3.3 | CHO compounds

Double-bond equivalence (DBE) is used to determine the number of rings plus the number of double bonds or triple bonds to carbon atoms. For a given formula of $C_cH_hO_o$, its DBE can be calculated from the following Equation 1:

$$DBE = (2c + 2 - h)/2 \qquad (1)$$

where c and h represent the number of carbon and hydrogen atoms in the molecule, respectively. In this work, the DBE value of a given compound molecule was directly calculated from the assigned formula. It should be noted that negative-ion ESI mainly produces deprotonated ions, resulting in half-integer DBE values. Thus, the DBE values reported were subtracted from the calculated values by 0.5 to the corresponding neutral molecules. There were 82 and 61 compounds with DBE $\leq$ 2 in the copal resin and amber, respectively, accounting for only 2.03% and 2.21%, respectively, of the total. The DBE values for 97.97% and 97.79% of the identified compounds in the two samples were greater than 2, and their relative abundances were 99.65% and 99.44%, respectively.

Figure 3 shows the relative abundance of the O_x class with different DBE values in the DCM extracts of the amber and copal resin by negative-ion ESI FT-ICR MS. The relative abundance was calculated by excluding the isotopic peaks in the mass. O_1–O_{20} class species were detected in both the amber and copal resin extracts, whereas only trace quantities of O_1 and O_{17}–O_{20} species were detected. The O_4–O_{12} class species were the main components in both extracts.

However, the copal resin had a higher abundance of low-oxygen compounds than the amber. The copal resin extract had the highest relative abundance of the O_5–O_7 class species, whereas the O_9–O_{10} class species were the dominant component in the amber extract. The abundance of compounds with the same DBE is closely related to the number of oxygen atoms. Generally, with the increasing number of oxygen atoms, the DBE increased and the abundance of those compounds with high DBE also increased. For some O_{12}–O_{20} compounds, the maximum DBE reached 15 or higher (not shown in Figure 3). Although each O_x class had a different relative abundance in the copal resin and amber extracts, the DBE distribution in each O_x class was very similar, indicating that they had very similar compositions and sources. In both extracts, the relative abundance of a class compound with a DBE reached a maximum and then decreased as the number of oxygen atoms increased, except for compounds with DBE = 4 in the copal resin. For example, the highest relative abundance of the DBE = 5 compounds was achieved when the oxygen atom number was six (O_6 class species); the relative abundance then gradually decreased. The relative abundances of compounds with the same DBE were different in both extracts. For example, the relative abundances of low-DBE compounds (DBE = 2–6) in the copal resin were higher than those in the amber, whereas those of the relatively high DBE compounds (DBE = 7–12) exhibited the opposite trend. These characteristics indicate that the amber had a higher unsaturation and denser molecular structure than the copal resin, which is related to the higher maturity of amber.

The O_2 species in the copal resin and amber had similar distributions with carbon numbers spread between 13 and 20 and DBE = 3–6. The most abundant component in the extracts was $C_{20}H_{34}O_2$ (DBE = 4), which accounted for more than 60% of the O_2 species. This component may be a diterpenoid acid with four isoprene C_5 structures, which is the main nonvolatile component of copal resin
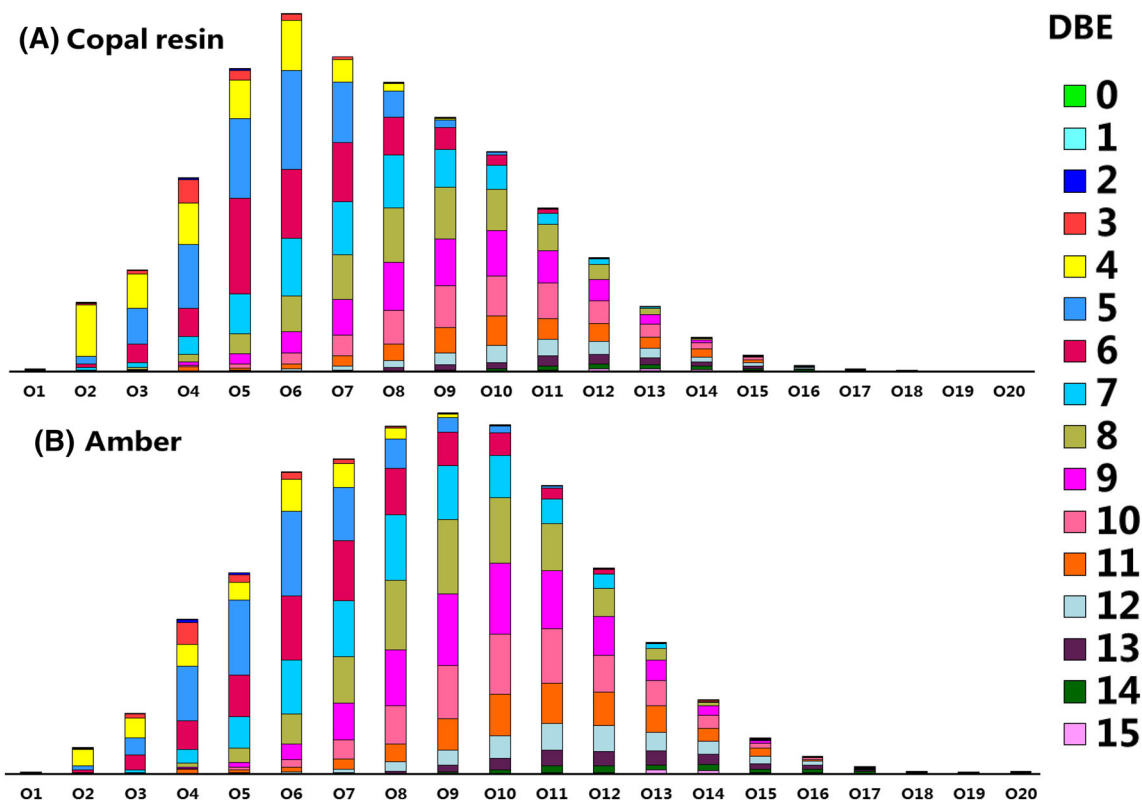
FIGURE 3 O_x species distributions and relative abundances in the DCM extracts of the copal resin and amber

and amber.[33] Compared to traditional GC–MS analysis, the detected compounds had less relative oxygen abundance, indicating that FT-ICR MS focused on a higher degree of polarisation compounds.[15] For the O_3 species, the copal resin extract contained more compounds than the amber extract. The most abundant compounds for this species in the copal resin and amber were $C_{20}H_{32}O_3$ (24.71%, DBE = 5) and $C_{15}H_{22}O_3$ (15.91%, DBE = 6), respectively. The C_{15} compound in the O_3 species may be a kind of polymer formed by the dehydration of succinic acid. Its higher relative content indicated a higher degree of polymerisation in the amber than in the copal resin, which may have been caused by the thermal conversion from copal resin to amber.[34]

Figure 4 and 5 show the plots of DBE vs. carbon number for the O_{4-12} class species in the copal resin and amber extracts, respectively. The area of each circle indicates the abundance (the ion signal) for each assigned compound. They have some characteristics in common. For example, the abundances of C_{10}–C_{20} compounds were obviously dominant when the number of oxygen atoms was low (O_4–O_7), whereas C_{30}–C_{40} was the main component of the O_8–O_{12} class species. Similarly, the abundances of DBE = 4–6 compounds had advantages in the O_4–O_7 class, whereas the DBE = 8–11 species dominated in the O_8–O_{12} class.

However, the differences between the two DCM extracts are also obvious. In the copal resin, the dominant O_4 components are C_{20} species (Figure 4), such as $C_{20}H_{32}O_4$ (13.64%, DBE = 5) and $C_{20}H_{34}O_4$ (12.52%, DBE = 4). These are likely dimers of succinic acid

with different degrees of hydrogenation. In the amber, the C_{15} species were the two compounds with the highest relative abundance, where $C_{15}H_{22}O_4$ (DBE = 5) accounted for 13.6% and $C_{15}H_{20}O_4$ (DBE = 6) accounted for 9.24%. For the O_5 to O_7 classes, the C_{15} and C_{20} species had similar abundance distributions, that is, $C_{15} > C_{20}$ in the amber, whereas $C_{15} < C_{20}$ in the copal resin. The exact molecular structures of these compounds cannot be determined at present. A notable difference of C_5H_8 presented by the series of plots suggests isoprene as the main structural backbone in the amber and copal resin. These structural features are consistent with the GC–MS and Py-GC–MS results.[15] The C_{15} species lack a basic isoprene structure as compared to the C_{20} species, which was likely lost during thermal evolution from copal resin to amber.

For the O_8 classes, there were two obviously abundant dominant groups on the dot diagrams of the two samples. The difference is that they were mainly distributed in C_{15}–C_{20} (DBE = 5–7) and C_{30}–C_{40} (DBE = 8–10) in the copal resin and in C_{15}–C_{20} (DBE = 5–7) and C_{25}–C_{35} (DBE = 7–11) in the amber. Moreover, the proportion of the dominant C_{25}–C_{35} group in the amber was obviously higher than that in the copal resin. For the O_9–O_{12} classes, compounds with high carbon numbers and high DBEs were dominant in the two samples. The copal resin was mainly composed of C_{30}–C_{40} (DBE = 7–11) compounds, whereas the amber was mainly composed of C_{25}–C_{35} (DBE = 8–12) species. For the O_{13+} classes, the most abundant compound class in the copal resin always had one less C_5 basic isoprene unit than that in the amber.
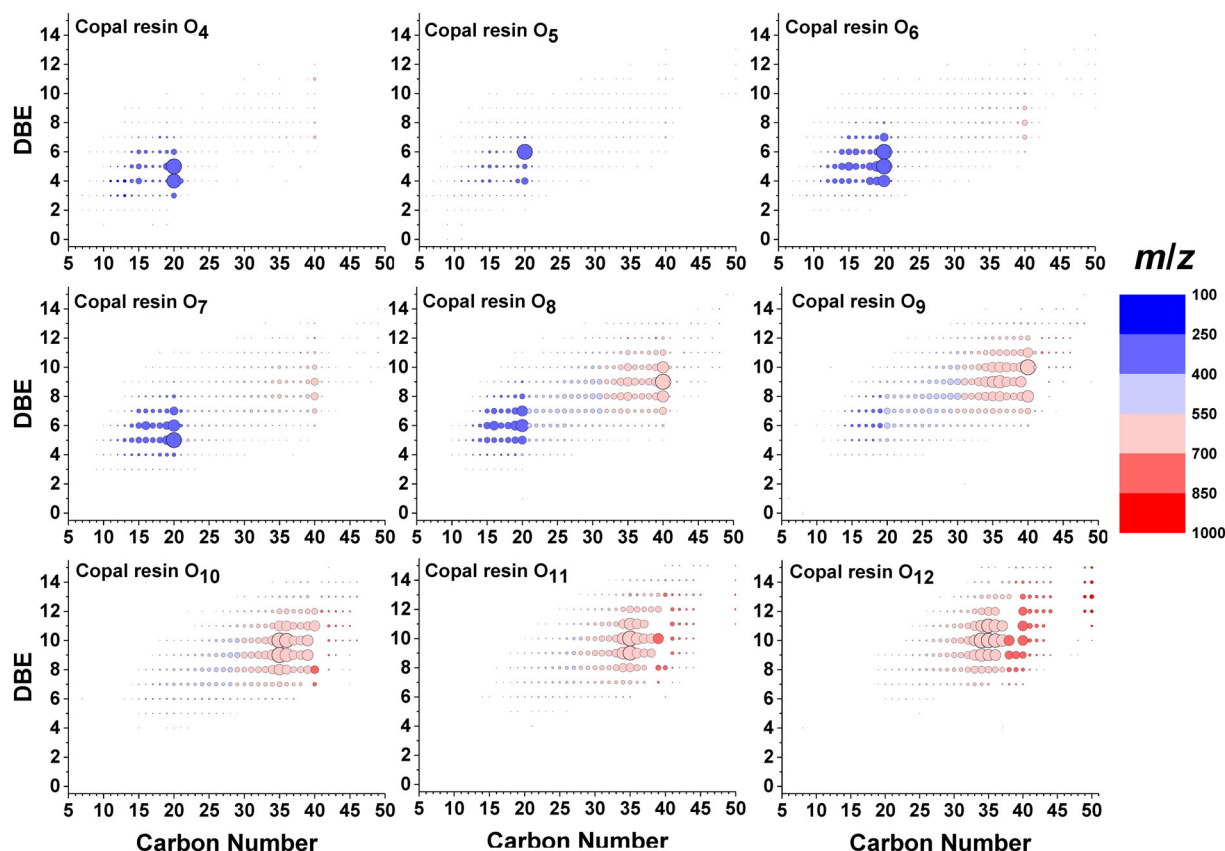
FIGURE 4 Iso-abundance plots of double-bond equivalence (DBE) versus carbon number distribution of O_4–O_{12} class species in the DCM extracts of the copal resin. The size of each circle is positively correlated to the ion abundance of each molecule

According to the composition and distribution of major-component CHO compounds, copal resin and amber have similar chemical components and structures, which indicate that they have similar origins. It can be inferred that the petrochemical process of converting copal resin to amber is accompanied by evaporation and dispersion of volatile molecules and polymerisation of relatively small molecules. Copal resin has a relatively low maturity. The mass fraction of unpolymerised volatile components in the copal resin was higher than that in the amber. With increasing maturity, the unsaturated C=C double bond in the copal resin is continuously broken. However, the isoprene C_5 basic structural unit linked by unsaturated bonds falls off and volatilises. Thus, the most abundant compounds in copal resin comprised more than one C_5 basic unit as compared to amber for the O_{3+} class species, as shown in Figure 4 and 5. However, the molecule polymerises to form polycyclic polymers with larger molecular weights and more carbon and oxygen atoms, and thus the relative abundances of compounds with a high number of carbon and oxygen atoms in amber were higher than those in copal resin (Figure 3).

3.4 | Average molecular formula for O_x class species

The DBE value with significant abundance for a given class varied in accordance with the number of oxygen atoms. The magnitude-weighted DBE (DBE_{av}), used to describe the overall DBE distribution, is defined as follows:

$$DBE_{av} = \frac{\sum_i li \times (DBE)i}{\sum_i li} \quad (2)$$

where l_i and $(DBE)_i$ are the abundance and DBE value of peak i, respectively.[35] The DBE_{av} values are presented in Table 2; they increase with the number of oxygen atoms obtained from the formula of the oxygen compounds from the extracts of the copal resin and amber (Figure 6). The selected O-containing compounds shown in Figure 6 were the O_3–O_{15} class species, which had relative abundances greater than 3% in the two samples. Linear regression analysis showed a high degree of linearity of the data, with R^2 values of 0.9872 and 0.9881, respectively, suggesting strong correlations between the DBE_{av} values and the number of oxygen atoms in both samples. The positive correlation indicates that oxygen atoms contribute to the overall DBE of oxygen-containing compounds. However, the oxygen atom in the alcohol or ether functional group does not contribute to the DBE of the compound molecule. Thus, the oxygen atoms of the formulas in the copal resin and amber are probably in the form of carbonyl and/or carboxyl groups, which contain one or two oxygen atoms and one double bond. The molecules with more oxygen atoms are likely to contain more carboxyl or carbonyl groups.
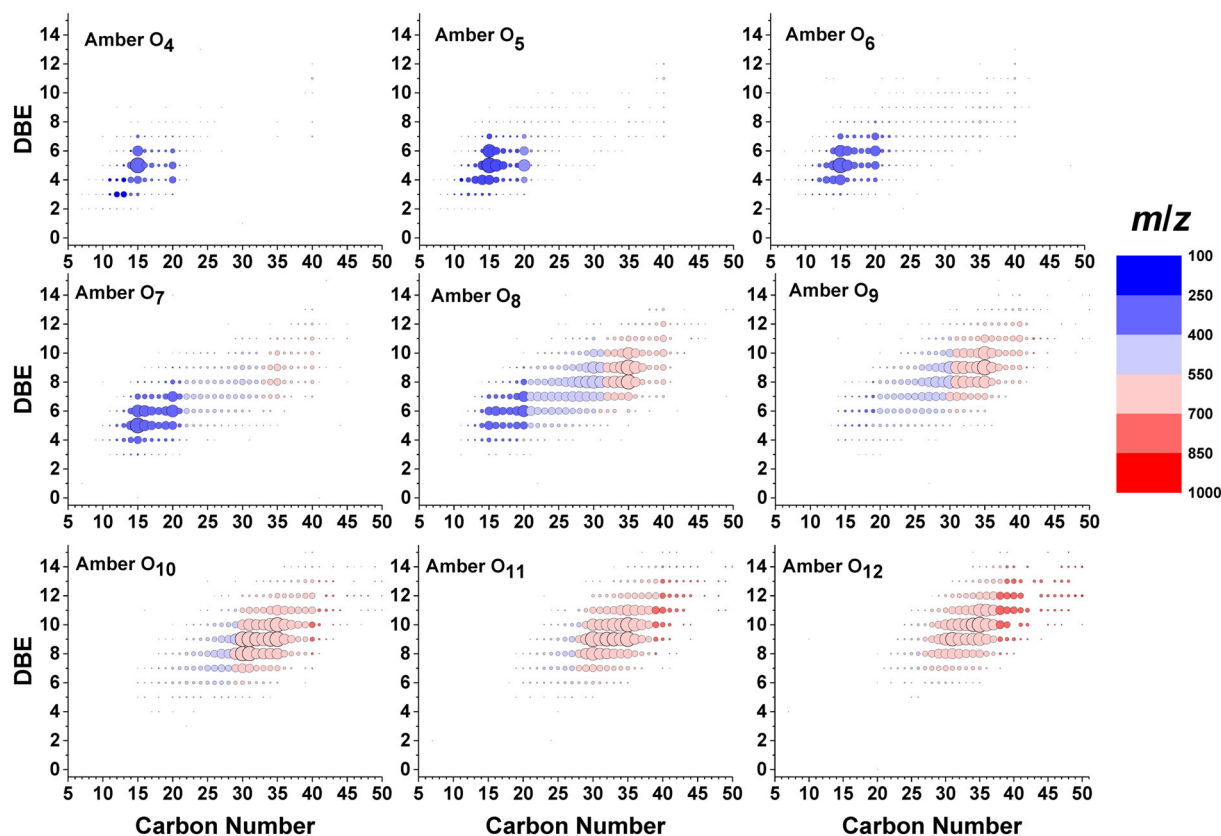
FIGURE 5 Iso-abundance plots of double-bond equivalence (DBE) versus carbon number distribution of O_4–O_{12} class species in the DCM extracts of the amber. The size of each circle is positively correlated to the ion abundance of each molecule

TABLE 2 Average of carbon number, hydrogen number, DBE and molecular formula for O_x class species in the copal resin and amber

Type	Copal resin				Amber			
	C_{av}	H_{av}	DBE_{av}	MF_{av}	C_{av}	H_{av}	DBE_{av}	MF_{av}
O_3	18.45	29.10	4.89	$C_{18}H_{29}O_3$	16.86	25.77	4.97	$C_{17}H_{26}O_3$
O_4	18.84	29.68	5.00	$C_{19}H_{30}O_4$	16.83	25.56	5.05	$C_{17}H_{26}O_4$
O_5	19.44	30.04	5.43	$C_{19}H_{30}O_5$	17.75	26.69	5.41	$C_{18}H_{27}O_5$
O_6	21.28	32.61	5.98	$C_{21}H_{33}O_6$	19.95	29.87	6.02	$C_{20}H_{30}O_6$
O_7	25.26	38.59	6.96	$C_{25}H_{39}O_7$	24.35	36.77	6.97	$C_{24}H_{37}O_7$
O_8	29.33	44.84	7.91	$C_{29}H_{45}O_8$	28.12	42.58	7.83	$C_{28}H_{43}O_8$
O_9	31.76	48.12	8.70	$C_{32}H_{48}O_9$	30.47	45.90	8.52	$C_{30}H_{46}O_9$
O_{10}	33.11	49.70	9.26	$C_{33}H_{50}O_{10}$	32.16	48.18	9.07	$C_{32}H_{48}O_{10}$
O_{11}	34.09	50.58	9.80	$C_{34}H_{51}O_{11}$	33.35	49.51	9.60	$C_{33}H_{50}O_{11}$
O_{12}	35.45	52.32	10.29	$C_{35}H_{52}O_{12}$	34.54	51.01	10.04	$C_{35}H_{51}O_{12}$
O_{13}	36.39	53.19	10.80	$C_{36}H_{53}O_{13}$	36.07	52.92	10.61	$C_{36}H_{53}O_{13}$
O_{14}	37.88	55.02	11.37	$C_{38}H_{55}O_{14}$	37.53	54.61	11.22	$C_{38}H_{55}O_{14}$
O_{15}	38.78	55.70	11.94	$C_{39}H_{56}O_{15}$	38.85	56.80	11.45	$C_{39}H_{57}O_{15}$

The subtraction or addition of multiple carbonyl and/or carboxyl groups without a significant change in the core molecular structure would result in a slope of 0.5 for the linear relationship between DBE and the number of oxygen atoms.[36] The slopes and y-intercepts can also be obtained using the linear equation of regression analysis (Figure 6). The slopes for the copal resin and amber were 0.64 and 0.60, respectively, values that are close to 0.5, indicating that the addition or removal of two oxygen atoms will result in the compound

molecule increasing or decreasing one DBE value. A carboxyl group contains two oxygen atoms and a double bond, and a carboxylic acid contributes one DBE. Therefore, the molecular structures of the O_3–O_{15} class species in the two samples mainly contained carboxylic acid heteroatom functional groups.

The intercepts of the linear relationship between DBE and the number of oxygen atoms indicate the DBE_{av} values of the core structures of ions with no oxygen atoms.[36] The y-intercepts
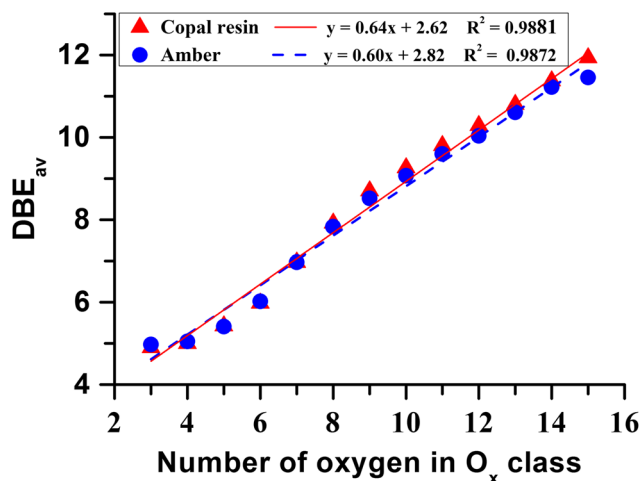
FIGURE 6 Linear regression of double-bond equivalence (DBE$_{av}$) versus the oxygen atoms number in O$_x$ class species

calculated were 2.62 and 2.82 for the copal resin and amber, respectively. It can be inferred that the average DBE value of the core carbon structure for the corresponding neutral compounds would be 2.12 and 2.32, respectively. Thus, it can be concluded that the core carbon structure contains at least two double bonds or rings. That is to say, the core molecular structure of the oxygen-containing compounds in the two samples included three double bonds or rings, consistent with the fact that most of the detectable CHO species had a DBE $\geq$ 3. One of the molecules satisfying the core structure condition is C$_5$ pentadienoic acid. It is also considered to be the basic structure of terpenoid resins, which is one of the main plant species that form amber. The similar slopes and intercepts of the copal resin and amber indicate that the main oxygenised compounds have similar chemical structures, proving that similar biogenic compounds can be deduced.

The overall carbon number distribution, defined as the average carbon number (C$_{av}$), was also calculated using an equation similar to Equation 2.

$$C_{av} = \frac{\sum_i li \times (no.of\ C)i}{\sum_i li} \qquad (3)$$

In the Equation 3, (no. of C) is the carbon number of peak i. The C$_{av}$ values of the oxygenised species of the copal resin and amber extracts are shown in Table 2. The table also lists the average hydrogen atom number for the O$_x$ class species, which was calculated from the DBE definition Equation 1,

$$H_{av} = 2\,C_{av} + (2 - 2\,DBE_{av}) \qquad (4)$$

Therefore, the average molecular formula (MF$_{av}$) can be expressed after the H$_{av}$ and C$_{av}$ are determined (Table 2). As shown in Table 2, for the O$_x$ class species in the extracts of the copal resin

and amber samples, both C$_{av}$ and H$_{av}$ increased with the increasing number of oxygen atoms. This finding indicates that the main contributors to the DBE$_{av}$ values were the oxygen atoms present in the carboxyl group. The new carbon chain was increased in the form of C=O.

4 | CONCLUSIONS

Copal resin and amber are complex mixtures with different evolutionary stages of plant resin. In this study, the DCM dissolved organic matter of two natural samples from Columbia, a copal resin and amber, were analysed by negative-ion ESI FT-ICR MS. The overall distribution patterns of the spectra and the approximate multiple relationships of molecular weight between the front and back peak groups indicated the presence of polymers in the samples. The CHO classes were detected as the dominant species while no S-containing compounds and very few N-containing compounds both in the polar fraction of the copal resin and amber. The analysis indicates a similar chemical compositions and plant origins for the copal and amber, being expected to be a useful tool in chemotaxonomy.

The CHO class distribution indicates that the petrochemical process of converting copal resin to amber was accompanied by evaporation and dispersion of volatile molecules and polymerisation of relatively small molecules. Thus, the most abundant compounds in copal resin comprised more than one C$_5$ basic unit as compared to amber, and the relative abundances of compounds with a high number of carbon and oxygen atoms in the amber were higher than those in the copal resin. The DBE$_{av}$ analysis of the Ox species suggested a C$_5$ pentadienoic acid as a core structure for the heteroatom compounds in copal and amber and the oxygen atom contributed to the overall DBE mainly by carboxylic acid heteroatom functional group.

CONFLICT OF INTEREST

We declared that we have no conflicts of interest to this work.

AUTHOR CONTRIBUTORS

Yankuan Tian completed the experiments, processed and analysed the data and drafted the manuscript. Zhao-Wen Zhan designed the experiments and finalised the work. Jia-Nan Sun and Bin Jiang processed the samples and assisted in some experiments.

ORCID

Yankuan Tian https://orcid.org/0000-0002-8882-3989

REFERENCES

1. Anderson KB. The nature and fate of natural resins in the geosphere XII. Investigation of C-ring aromatic diterpenoids in Raritan amber by pyrolysis-GC-matrix isolation FTIR-MS. *Geochem Trans*. 2006;7:1-9.

2. Edwards HGM, Farwell DW, Jorge Villar SE. Raman microspectroscopic studies of amber resins with insect inclusions. *Spectrochim Acta a*. 2007;68(4):1089-1095.

3. Martinez-Richa A, Vera-Graziano R, Rivera A, Joseph-Nathan P. A solid-state ^{13}C NMR analysis of ambers. *Polymer*. 2000;41(2): 743-750.

4. Brody RH, Edwards HGM, Pollard A. A study of amber and copal samples using FT-Raman spectroscopy. *Spectrochim Acta a: Mol Biomol Spectrosc*. 2001;57(6):1325-1338.

5. Barone G, Capitani D, Mazzoleni P, et al. ^{13}C solid state nuclear magnetic resonance and μ-raman spectroscopic characterization of sicilian amber. *Appl Spectrosc*. 2016;70(8):1346-1355.

6. Beck CTW, Wilbur E, Meret S. Infra-red spectra and the origin of amber. *Nature*. 1964;201(4916):256-257.

7. Lambert JB, Frye JS, Poinar GO. Amber from the Dominican Republic: analysis by nuclear magnetic resonance spectroscopy. *Archaeometry*. 1985;27(1):43-51.

8. Lambert JB, Johnson SC, Poinar GO, Frye JS. Recent and fossil resins from New Zealand and Australia. *Geoarchaeology*. 1993;8(2):141-155.

9. Lambert JB, Tsai CYH, Shah MC, Hurtley AE, Santiago-Blay JA. Distinguishing amber and copal classes by proton magnetic resonance spectroscopy. *Archaeometry*. 2012;54(2):332-348.

10. Grantham PJ, Douglas AG. The nature and origin of sesquiterpenoids in some tertiary fossil resins. *Geochim et Cosmochim ac*. 1980;44(11): 1801-1810.

11. Otto A, Simoneit BRT, Wilde V, Kunzmann L, Püttmann W. Terpenoid composition of three fossil resine from cretaceous and tertiary conifers. *Rev Palaeobotany Palynol*. 2002;120(3-4):203-215.

12. Virgolici M, Ponta C, Manea M, et al. Thermal desorption/gas chromatography/mass spectrometry approach for characterization of the volatile fraction from amber specimens: a possibility of tracking geological origins. *J Chromatogr a*. 2010;1217(12): 1977-1987.

13. Sonibare OO, Hoffmann T, Foleyb SF. Molecular composition and chemotaxonomic aspects of Eocene amber from the Ameki formation, Nigeria. *Org Geochem*. 2012;51:55-62.

14. Dutta S, Mallick M, Kumar K, Mann U, Greenwood PF. Terpenoid composition and botanical affinity of Cretaceous resins from India and Myanmar. *Int J Coal Geol*. 2011;85(1):49-55.

15. Anderson KB, Winans RE, Botto RE. The nature and fate of natural resins in the geosphere-II. Identification, classification and nomenclature of resinites. *Org Geochem*. 1992;18(6):829-841.

16. Pereira R, Carvalho I d S, Simoneit BRT, Azevedo D d A. Molecular composition and chemosystematic aspects of cretaceous amber from the Amazonas, Araripe and Recôncavo basins, Brazil. *Org Geochem*. 2009;40:863-875.

17. Bray PS, Anderson KB. The nature and fate of natural resins in the geosphere XIII: a probable pinaceous resin from the early Cretaceous (Barremian), Isle of Wight. *Geochem Trans*. 2008;9:1-5.

18. Marshall AG, Hendrickson CL, Ernmetta MR, Rodgers RP, Blakney GT, Nilsson CL. Fourier transform ion cyclotron resonance: state of the art. *Eur J Mass Spectrom*. 2007;13(1):57-59.

19. Shi Q, Pan N, Long H, et al. Characterization of middle-temperature gasification coal tar. part 3: molecular composition of acidic compounds. *Energ Fuel*. 2012;27:108-117.

20. Kujawinski EB, Behn MD. Automated analysis of electrospray ionization fourier transform ion cyclotron resonance mass spectra of natural organic matter. *Anal Chem*. 2006;78(13):4363-4373.

21. Wang L, He C, Zhang Y, et al. Characterization of acidic compounds in heavy petroleum resid by fractionation and negative-ion electrospray ionization Fourier transform ion cyclotron resonance mass spectrometry analysis. *Energ Fuel*. 2013;27(8):4555-4563.

22. Lu J, Zhang Y, Shi Q. Ionizing aromatic compounds in petroleum by electrospray with $HCOONH_4$ as ionization promoter. *Anal Chem*. 2016;88(7):3471-3475.

23. Pan Y, Liao Y, Shi Q. Variations of acidic compounds in crude oil during simulated aerobic biodegradation: monitored by semiquantitative negative-ion ESI FT-ICR MS. *Energ Fuel*. 2017;31(2):1126-1135.

24. Simoneit BRT, Mazurek MA. Organic matter of the troposphere II—natural background of biogenic lipid matter in aerosols over the rural western United States. *Atmos Environ*. 1982;16(9):2139-2159.

25. Koch BP, Dittmar T. From mass to structure: an aromaticity index for high-resolution mass data of natural organic matter. *Rapid Commun Mass Sp*. 2006;20(5):926-932.

26. Willoughby AS, Wozniak AS, Hatcher PG. A molecular-level approach for characterizing water-insoluble components of ambient organic aerosol particulates using ultrahigh-resolution mass spectrometry. *Atmos Chem Phys*. 2014;14(18):10299-10314.

27. Lu Y, Li X, Mesfioui R, et al. Use of ESI-FTICR-MS to characterize dissolved organic matter in headwater streams draining forest-dominated and pasture-dominated watersheds. *Plos One*. 2015;10(12):1-21, e0145639. https://doi.org/10.1371/journal.pone.0145639

28. Antony R, Grannas AM, Willoughby AS, Sleighter RL, Thamban M, Hatcher PG. Origin and sources of dissolved organic matter in snow on the East Antarctic ice sheet. *Environ Sci Technol*. 2014;48(11): 6151-6159.

29. He ZQ, Sleighter RL, Hatcher PG, et al. Molecular level comparison of water extractives of maple and oak with negative and positive ion ESI FT-ICR mass spectrometry. *J Mass Spectrom*. 2019;54(8):655-666.

30. Czechowski F, Simoneit BRT, Sachanbinski M, Chojcan J, Wolowiec S. Physicochemical structural characterization of ambers from deposits in Poland. *Appl Geochem*. 1996;11(6):811-834.

31. Scalarone D, Lazzari M, Chiantore O. Ageing behaviour and analytical pyrolysis characterisation of diterpenic resins used as art materials: Manila copal and sandarac. *J Anal Appl Pyrol*. 2003;68:115-136.

32. McCoy VE, Gabbott SE, Penkman K, et al. Ancient amino acids from fossil feathers in amber. *Sci Rep*. 2019;9:1-8.

33. Grimalt JO, Simoneit BRT, Hatcher PG, Nissenbaum A. The molecular composition of ambers. *Org Geochem*. 1988;13(4-6):677-690.

34. Guiliano M, Asia L, Onoratini G, Mille G. Applications of diamond crystal ATR FTIR spectroscopy to the characterization of ambers. *Spectrochim Acta a*. 2007;67(5):1407-1411.

35. Liu Y, Shi Q, Zhang YH, et al. Characterization of red pine pyrolysis bio-oil by gas chromatography-mass spectrometry and negative-ion electrospray ionization Fourier transform ion cyclotron resonance mass spectrometry. *Energ Fuel*. 2012;26(7):4532-4539.

36. Bae E, Yeo IJ, Jeong B, Shin Y, Shin KH, Kim S. Study of double bond equivalents and the numbers of carbon and oxygen atom distribution of dissolved organic flatter with negative-mode FT-ICR MS. *Anal Chem*. 2011;83:4193-4199.

SUPPORTING INFORMATION

Additional supporting information may be found online in the Supporting Information section at the end of this article.